

## Chapter 2

# Spectroscopic Parameters in Nuclear Magnetic Resonance

**Abstract** In common with other spectroscopic techniques, NMR measures the intensities of the nuclear spin transitions versus the frequencies at which these transitions happen. In this chapter, the spectroscopic parameters of NMR will be described, some of which are shared by other spectroscopies while others are unique to the technique, arising from the properties described in the previous chapter. The origin and physical characteristics of the chemical shift, the spin–spin scalar coupling and the nuclear Overhauser effect (NOE) will be introduced here.

**Keywords** Chemical shift • Coupling constant • Multiplets • Nuclear Overhauser Effect (NOE) • Relaxation

### 2.1 The Chemical Shift and the Spectral Intensity

The NMR frequency of any particular nucleus is *spectrometer dependent*, that is, carries with it the effect of the static field applied ( $B_0$ ), which is the origin of the split levels that generate the NMR effect (Chap. 1). In order to be able to compare spectra recorded at different field strengths we need to define other parameters. The chemical shift parameter ( $\delta$ ) is central to the interpretation of NMR spectra, and it is equivalent in importance to the frequency, wavenumber or wavelength used in other spectroscopies such as IR, CD, UV absorbance or fluorescence.

#### 2.1.1 The Shielding Screening Constant

The basic equation in NMR described in Chap. 1,  $\omega = \gamma B_0$ , tells us that when any type of nucleus in the sample is subjected to the same external magnetic field,  $B_0$ , it will experience the corresponding Larmor frequency (according to its  $\gamma$ ). Therefore, the NMR spectrum will be composed of identical resonance lines of the

same frequency for a particular type of nucleus. Fortunately for our purposes, this is not the case experimentally and each nucleus resonates with a particular frequency. To show this point, we consider as an example a simple molecule such as ethanol ( $\text{CH}_3\text{CH}_2\text{OH}$ ) that would present an “ideal” proton NMR spectrum as that shown in Fig. 2.1 (main panel). Three groups of signals can be clearly differentiated (their splitting is discussed later in this chapter), corresponding to the chemical differences of the hydrogen atoms in the molecule: one group of signals corresponds to the methyl group ( $-\text{CH}_3$ ), a second one to the methylene protons ( $-\text{CH}_2-$ ) and a third for the hydroxyl group ( $-\text{OH}$ ). Chemically speaking, it is obvious that each group of hydrogens in the ethanol molecule has different molecular environments, and therefore will experience slightly different local fields. If we compare the frequency for each  $^1\text{H}$  nucleus in ethanol with that calculated by  $\gamma B_0$ , we find that each resonance frequency measured experimentally is different from the theoretically predicted one. That is, any of the resonance frequencies observed can be described as:

$$\omega = \gamma B_0 - \sigma \gamma B_0 = \gamma B_0(1 - \sigma)$$

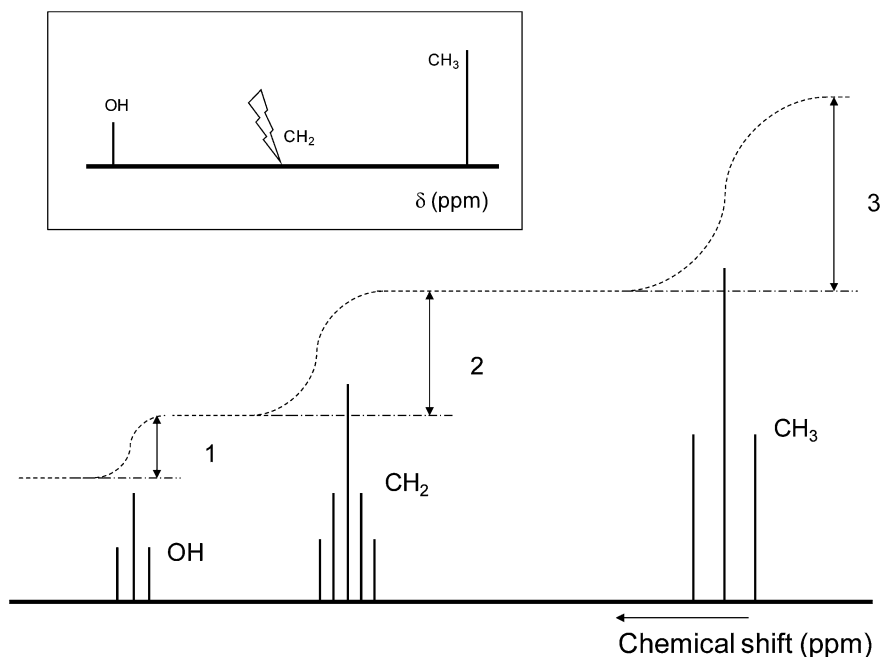


**Fig. 2.1** NMR spectrum of ethanol. Schematic representation of the  $^1\text{H}$  spectrum of ethanol. The dotted line indicates the integral of the signals which correlates with the number of equivalent protons. Inset: spectrum of ethanol when the  $\text{CH}_2$  resonance is irradiated (the bolt) causing the decoupling of the rest of signals (Sect. 2.2.4)

where the factor  $\sigma$  is called the *shielding* (or *screening*) *constant*.  $\sigma$  can be positive or negative depending on whether the local field adds or subtracts from the applied field. The  $\sigma$  constant varies with  $B_0$  along the axes (x, y and z) within the molecule, and can be described mathematically as a tensor. Since  $\sigma$  varies with the chemical environment, identical atoms within a molecule (i.e. the different protons in ethanol) will resonate at different frequencies and therefore render unique NMR signals, giving rise to the richness and power of NMR spectroscopy.

It is not possible to calculate the precise value of  $\sigma$  for any given nucleus in any molecule due to the different mechanisms at work. However, we can try to understand the variation within molecules by considering the different types of effects that contribute to it:

$$\sigma = \sigma_d + \sigma_p + \sigma_m + \sigma_{rc} + \sigma_{ef} + \sigma_{sol} + \sigma_{ps}$$

The contributions are from local diamagnetism ( $\sigma_d$ ), local paramagnetism ( $\sigma_p$ ), neighbouring anisotropy ( $\sigma_m$ ), ring-currents ( $\sigma_{rc}$ ), electric field ( $\sigma_{ef}$ ), solvent contribution ( $\sigma_{sol}$ ) and the effect due to the presence of paramagnetic species ( $\sigma_{ps}$ ). The origin and effect of each one of these screening constant contributions is described in the following.

### 2.1.1.1 The Diamagnetic Contribution

Every atomic nucleus is surrounded by an electron cloud (except  $H^+$ ). The presence of an external  $B_0$  causes the electrons to precess about the axis of the field, creating a current that gives rise to its own small magnetic field (Fig. 2.2a). The  $\sigma_d$  contribution can be calculated from the value of the scalar product of the electron-nucleus distance and the electron orbital density. The diamagnetic effect describes the behaviour of spherically distributed electronic clouds, such as the s-orbital in protons. Therefore, its effect is particularly important in hydrogen atoms (so called *protons* or  $^1H$  in NMR jargon), but not that relevant in heavier nuclei. It is also affected by the presence of other nuclei withdrawing or donating electronic charge, that is, by alterations in the electron clouds. Thus, highly electronegative nuclei, like oxygen or nitrogen, will withdraw electronic charge, with the effect of deshielding nearby hydrogen atoms. A case in point is the downfield (deshielded) resonance of the  $^1H$  at the C1 position in glucose due to the high electronegativity of the nearby ring oxygen.

Even in hydrogen, the distribution of electrons is usually non-spherical, and the shielding depends on the orientation with respect to  $B_0$ . In  $sp^3$  carbons, protons are tetrahedrally bonded and the electron distribution is invariable upon rotation. On the other hand, for  $sp^2$  carbons (e.g.  $C=C$ ,  $C=O$  groups) the shielding depends highly on the orientation of the bond relative to  $B_0$ . Due to this anisotropy, the effective field that the nuclei actually experience can deviate with the direction of  $B_0$ , and different directions of the field will result in different resonance positions for the same chemical species. This effect is known as *chemical shift anisotropy*

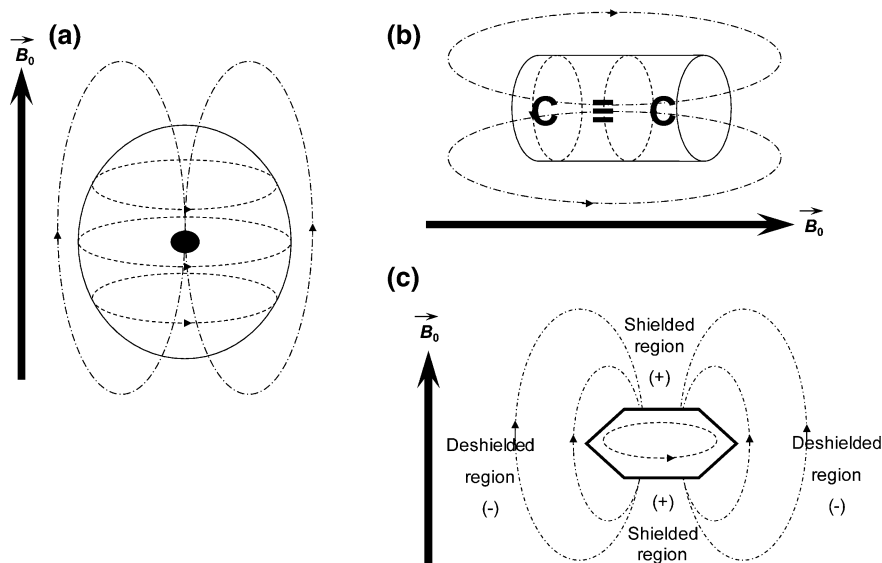


**Fig. 2.2** Contributions and effects of the shielding parameter. **a** Diamagnetic effect: the *dashed lines* indicate the movement of the electron within its orbital (large continuous circle); the *dot-and-dashed lines* indicate the magnetic field created by the electronic current; the *filled circle* represents the nucleus. The direction of the external magnetic field is shown by an arrow on the left-side of the figure. **b** Magnetic anisotropy of a triple bond: only the carbons of the triple bond are shown. The *dashed lines* indicate the movement of the electrons within the triple bond; the *dot-and-dashed lines* indicate the field created by the electronic current of the triple bond. The direction of the external magnetic field is indicated by an arrow at the bottom of the figure. **c** Ring-current effect: the *dot-and-dashed lines* indicate the direction of the magnetic field created by the ring-current. The dashed line on the ring shows the movement of the electrons in the aromatic plane. Shielded and deshielded regions are indicated. The external magnetic field is indicated by an arrow on the left side of the figure (this panel has been adapted from Structural Virology book by Springer, with permission)

(CSA). In solids, where molecular rotation is hindered, the line width of each resonance is significantly broadened due to the CSA. In liquids, where rotation is not hampered, CSA contributes to the relaxation of spins (Chap. 1) and is, in fact, the major relaxation mechanism for non-protonated carbons.

### 2.1.1.2 The Paramagnetic Contribution

The circulation of electrons around p-orbitals induced by external magnetic fields causes deshielding (downfield shifts) of the nearby nuclei. The paramagnetic term can be calculated if the way in which the electron wave-functions are altered by the presence of the other nuclei is known. The shifts caused by the paramagnetic contribution are much larger than for the diamagnetic effect, and this contribution is the main source for chemical shift variation in all nuclei heavier than  $^1\text{H}$ .

### 2.1.1.3 Neighbour Anisotropy and Ring-Current Effect Contributions

Some types of chemical bonds create an additional magnetic field which is anisotropic in space. A typical example is the carbon-carbon triple bond  $\text{C}\equiv\text{C}$  (Fig. 2.2b), where the  $\pi$  electrons form an electron cloud extending around the bond axis in the shape of a cylinder. The  $B_0$  forces the  $\pi$  electrons to rotate around the bond axis creating a magnetic field, which counteracts the static magnetic field.

The same effect is observed in the  $\pi$ -cloud of aromatic systems. In the presence of  $B_0$ , a planar aromatic ring with its delocalized  $\pi$  electrons “creates” its own magnetic field (Fig. 2.2c). A nucleus below or above the ring plane will be shielded from the external magnetic field, but it will be deshielded if it is located at other positions relative to the ring. Therefore, the magnitude of the total field experienced by a nucleus informs us on its orientation with respect to the ring. Such anisotropies can dramatically alter the shape of spectra, increasing the spread of signals across the chemical shift range. For instance in the case of proteins, the effects of the aromatic rings from amino acids like histidine, phenylalanine, tyrosine and tryptophan, can be used as indicators for the presence of protein structure: well-spread resonances are a sign of the close proximity of those aromatic rings to other residues, and consequently of a folded protein.

### 2.1.1.4 The Electric Field Contribution

Strongly polar groups create intramolecular electric fields, which distort the electron density in the rest of the molecule, influencing  $\sigma$ . The electric field effects account for the electron movement in the polar bond against the inherent electric field, and the asymmetry induced by this electronic shift. Electric fields are important, for example, in  $^{19}\text{F}$  resonances as well as in hydrogen-bonded protons. Hydrogen-bonds decrease the electron density at nearby chemical bonds, and lead to a high frequency resonance. In fact, hydrogen-bonded protons can be easily recognized by their shifted frequency, although this is highly dependent on experimental sample conditions like temperature, concentration and solvent.

### 2.1.1.5 The Solvent Contribution

The effects of solvents on the spectra of solutes can be manifested through several mechanisms. In the first place, aromatic solvents such as benzene or toluene will possess ring-current effects like those described before. Second, an orientation effect can be found when a polar molecule is dissolved in a polar solvent, producing an ordering of solvent molecules around the solute that alters the magnetic field experienced by the latter. A final effect is encountered when hydrogen-bonds are formed between the solute and the solvent.

### 2.1.1.6 The Contribution of Paramagnetic Compounds

Paramagnetic compounds are those that present unpaired electrons. Paramagnetic entities in an NMR sample give rise to signal broadening due to relaxation effects. The resonance frequency can also be influenced through Fermi-contact interactions (Sect. 2.2.1) between a nuclear spin and an unpaired electron from the paramagnetic species. There are several examples in the literature describing the use of paramagnetic compounds in NMR. For instance, the so-called *shift-reagents* are paramagnetic chemicals used with the purpose of dispersing previously overlapped resonances in order to clarify proton spectra (e.g. Cr(III) in Cr(acac)<sub>3</sub>). The paramagnetic contribution is also observed in the NMR spectra of some metal nuclei. In this type of atoms, the dipolar coupling between the nucleus and the electron can cause signal broadening, but if the coupling is much smaller than the relaxation rate of the electron, sharp lines with large resonance frequencies are observed in the NMR spectrum of the metal (*Knight shift*).

### 2.1.2 The Chemical Shift

To quantify the resonance frequencies, we need signal reference standards. The common standard for protons is the <sup>1</sup>H resonance of Si(CH<sub>3</sub>)<sub>4</sub> (tetramethylsilane, abbreviated as TMS), a chemically stable molecule that presents a unique <sup>1</sup>H resonance, which is very intense as it is contributed to by 12 equivalent proton atoms, to which the arbitrary value of 0 Hz frequency is assigned. Conveniently, the zero reference frequency for the <sup>13</sup>C nucleus is also that of the methyl carbon of TMS. Alternatively, the <sup>1</sup>H signal of the residual non-deuterated solvent in the sample (which has been previously referenced to TMS) can also be used as reference, like for instance CHCl<sub>3</sub> or DMSO ((CH<sub>3</sub>)<sub>2</sub>SO). For the H<sub>2</sub>O/D<sub>2</sub>O samples typically used in biomolecular NMR, <sup>1</sup>H resonances are normally referenced to (4,4-dimethyl-4-silapentane-1-sulfonic acid) DSS or (trimethylsilyl propionate) TSP, both resonating at 0 Hz. Each nucleus in the periodic table has its own chemical as NMR standard, although in biomolecules the common procedure to calibrate the <sup>13</sup>C and <sup>15</sup>N nuclei is to take into account the reference of <sup>1</sup>H (Wishart et al. 1995).

Even though a reference is used to calibrate the signals in the spectra, the separation in hertz of a particular resonance from the standard signal depends on the  $B_0$  at which they are recorded, as the higher the field the greater the separation between the energy levels and therefore the frequency of absorption (Chap. 1). To be consistent at any  $B_0$ , we define *chemical shifts*. The chemical shifts are dimensionless units reported on the  $\delta$  scale (in ppm), which is defined as  $\delta = ((\nu - \nu_0)/\nu_0) \times 10^6$ , where  $\nu_0$  is the resonance frequency of the standard,  $\nu$  is the frequency of the particular nucleus, and the  $10^6$  factor gives the scale of the magnitude in parts per million. NMR spectra are represented with the zero  $\delta$  in the

right-hand side of the frequency range, with increasing values towards the left side, an old remnant of early NMR experiments when spectra were acquired by continuously varying  $B_0$ . If  $\delta < 0$  the nucleus is considered shielded because the magnetic field it experiences is weaker than the field experienced by the nuclei in the standard compound. However, if  $\delta > 0$ , we say that the nucleus is deshielded because the local magnetic field is stronger than that experienced by the nuclei in the standard molecule under the same conditions. In general, the closer the nucleus is to an electronegative element, the more deshielded it will be (i.e. the larger its  $\delta$  value). The values of  $\delta$  can be used to make qualitative assessments about the presence of functional groups, in a similar fashion as functional group frequencies are identified in IR spectroscopy.

Based on the above arguments, several general statements can be made for interpreting proton spectra. Thus, in the aliphatic C–H bonds the shielding decreases in the series  $\text{CH}_3 > \text{CH}_2 > \text{CH}$ , with the methyl groups resonating around 0.9 ppm, while those corresponding to CH protons lay between 3.5 and 10.0 ppm (Fig. 2.3). There are some exceptions to this general rule, which occur when the observed proton is attached to an atom or group of atoms presenting high electronegativity. Aromatic protons appear between 6.0 and 8.0 ppm because, in addition to their  $\text{sp}^2$  hybridization, an extra deshielding contribution arises due to the ring-effects (Sect. 2.1.1.3). The resonance signals of protons belonging to aldehydes and carboxylic acids appear at very large  $\delta$  values ( $>8.5$  ppm). Carbon atoms bound to nitrogen, oxygen or halogens (very electronegative elements)

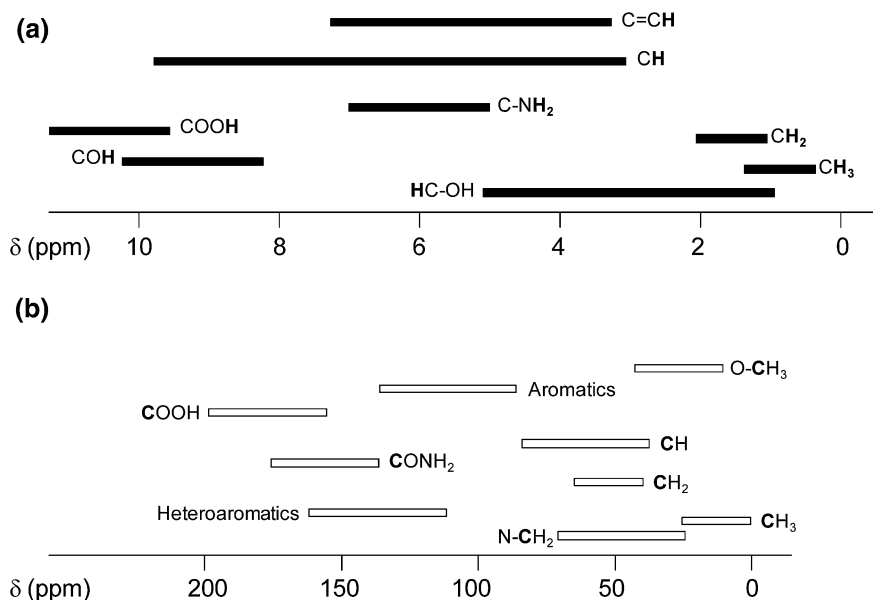


**Fig. 2.3** Resonance frequency ranges of characteristic chemical functional groups. **a**  $^1\text{H}$  chemical shifts. **b**  $^{13}\text{C}$  chemical shifts

induce large displacements in the resonance of neighbouring protons leading to deshielded chemical shifts (therefore, larger values). The NMR signals of labile protons like OH, NH, NH<sub>2</sub> and CO<sub>2</sub>H are concentration-, temperature- and solvent-dependent due to possible exchange reactions with the solvent (Fig. 2.3a) (Günther 1995).

These chemical shift rules can also be applied to <sup>13</sup>C. For instance, the chemical shifts of <sup>13</sup>C belonging to aliphatic chains are shielded (low  $\delta$ ), and those involved in aldehydes or acids are deshielded. However, since the  $\gamma$  of <sup>13</sup>C is different to that of <sup>1</sup>H (Table 1.2), the range of frequencies/chemical shifts is very different, with <sup>13</sup>C  $\delta$ s extending to above 200 ppm (Fig. 2.3b) (Günther 1995).

### 2.1.3 Signal Intensity

Each NMR signal encloses an area under the peak that can be quantified. As in any other spectroscopy, this area under the spectral curve correlates with the number of molecules or nuclei originating that transition. Together with the chemical shift information, we can use the relative intensities under each peak to determine which nucleus, or group of nuclei, give rise to a particular resonance; that is, we obtain structural and chemical characterization.

As an example, we shall use again the ethanol molecule. If we integrate with the adequate software the area under each peak, we should obtain relative intensities in the ratio 3:2:1 (Fig. 2.1, dashed line). The signal appearing more shielded (lowest  $\delta$ ) with a relative intensity of three correlates with the methyl (CH<sub>3</sub>) group. That with the relative intensity of two correlates with the CH<sub>2</sub> group and is deshielded compared to the methyl one due to the electronegative effect of the bound oxygen atom. The remaining signal integrating for one <sup>1</sup>H shows the largest  $\delta$  and corresponds to the O–H group.

## 2.2 The Scalar Coupling Constant

Any interaction that divides magnetically equivalent nuclei into two or more populations will cause its peaks in the NMR spectra to split. *Magnetic equivalent* nuclei are those presenting the same frequency (isochronous) and also identically coupled to any third nucleus. For instance, the protons of a methyl group are chemically and magnetically equivalent as a consequence of the free rotation about the C–C bond. All three protons have the same time-averaged chemical environment and hence the same frequencies. In contrast, *chemical equivalent* nuclei behave the same as one another chemically, they are also isochronous, but they can present different magnetic interactions to a third nucleus. All magnetic equivalent nuclei are also chemically equivalent, but the opposite is not necessarily true.



Two types of interaction between spins are known: *dipolar* and *scalar* coupling. The dipolar coupling depends on the orientation of the connecting vector between the two nuclei with respect to the static field (Chap. 1, Fig. 1.3a); this orientation changes rapidly in solution due to molecular tumbling, averaging the dipolar coupling to zero in isotropic (liquid) phase (although it can be observed in solid state and in liquid crystals). Therefore, it does not cause any possible splitting on the resonances in the solution state. On the other hand, the scalar coupling does not depend on molecular orientation but is transmitted through chemical bonds, inducing the splitting of resonances. This coupling will be described in detail in the following sections.

### 2.2.1 Spin–Spin Coupling

If we go back to the ethanol molecule (Fig. 2.1, main panel), its  $^1\text{H}$ -NMR spectrum shows splitting in its three resonances:  $\text{CH}_3$ ,  $\text{CH}_2$  and OH. Instead of a single sharp line for each of the three signals, the  $\text{CH}_3$  resonance appears as a triplet, as does the OH and the  $\text{CH}_2$  as a quintuplet. The fine structure of the NMR spectrum arises from the fact that each magnetic nucleus contributes to the local field experienced by its neighbours, slightly modifying their resonance frequencies. The strength of this interaction is proportional to the scalar product of the magnetic moments of both interacting nuclei, with a proportionality constant called the *coupling constant*, usually abbreviated to  $^nJ$  ( $n$  indicating the number of intervening covalent bonds). The  $J$  coupling is measured in hertz, is governed only by the magnetic moments of the nuclei involved, and is independent of the applied  $B_0$  (i.e.  $J$  will be identical for two coupled nuclei regardless of the NMR spectrometer used). The coupling is transmitted via the chemical bonds and, in general, its magnitude decreases with the distance (number of bonds) between the coupled nuclei. The strength of  $J$  also depends on the amount of overlap of the involved electron orbitals (Sect. 2.2.2).

To understand the effect of scalar coupling on NMR signals, consider a molecule that contains two spin- $1/2$  nuclei, A and X (Fig. 2.4). In the absence of scalar coupling, we have four levels depending on the orientations relative to the external magnetic field of the two spins: both oriented parallel or antiparallel, or one parallel and the other antiparallel, and the other way round. The transitions expected for the A nucleus (going from the  $\alpha$  state to the  $\beta$  state, with the X spin in either  $\alpha$  or  $\beta$  states) are drawn in Fig. 2.4a. The A nucleus will resonate at a certain frequency as a result of the external field and its inherent  $\sigma$ , giving rise to a single line for those two transitions. If there is a spin–spin coupling between the nuclei, the two states with both A and X spins presenting the same orientation (that is, either both nuclei in the  $\alpha$  or  $\beta$  state) will be destabilized (they will have more energy in the presence of the spin–spin coupling interaction), and the two states with the two A and X spins in alternate orientations will be stabilized. The final result will be that the two transitions for the A spin will have different energies and

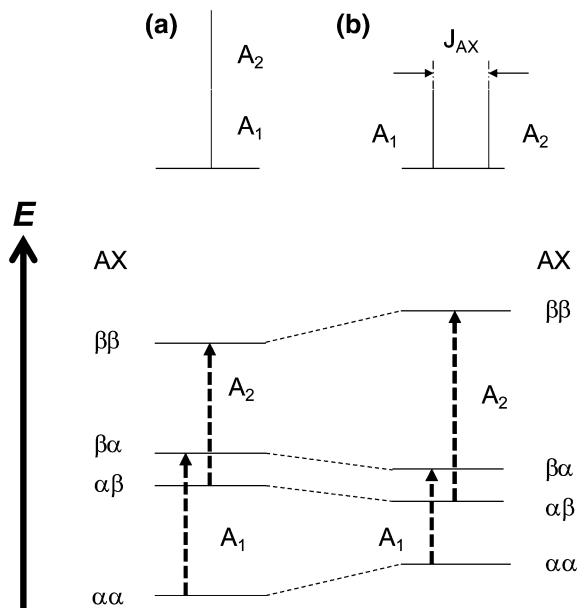


**Fig. 2.4** Nuclear energy levels for a two-spin system with spin  $1/2$ . Energy diagram without spin-spin coupling **a** and with coupling **b**. The parallel orientation of both spins was considered as the low-energy state. The levels  $\alpha\beta$  and  $\beta\alpha$  have the same energy (indistinguishable from a quantum perspective), but they are shown here with slightly different energies for the sake of distinguishing the  $A_1$  and  $A_2$  transitions. The  $A_1$  transition changes the state of the A nucleus from  $\alpha$  to  $\beta$  when the X state is  $\alpha$ ; the  $A_2$  transition changes the state of the A nucleus from the  $\alpha$  to  $\beta$  when X state is  $\beta$ . Therefore, in the spectrum for the A resonance, in the absence of coupling, a single peak appears corresponding to the sum of  $A_1$  and  $A_2$  (above on the *left* side). Note that the lengths of the *arrows* indicating the transitions  $A_1$  and  $A_2$  have equal length, because  $\alpha\beta$  and  $\beta\alpha$  are degenerate. In the presence of coupling, two peaks ( $A_1$  and  $A_2$ ), separated by  $J$ , correspond with the A nucleus (above on the *right* side). The same splitting would be observed for the X nucleus (not shown)

two lines will appear instead of the previous single resonance (Fig. 2.4b). The separation (in Hz) between the two lines forming a doublet is defined as the magnitude of the coupling  $J_{AX}$ . The same effect will be observed for the coupled spin X: two lines will appear instead of one, equally separated by  $J_{AX}$  Hz.

If a second A nucleus which is magnetically and chemically equivalent to the first (with the same chemical shift) is present in the molecule (Fig. 2.5a, (1)), the X resonance signal will be split into a doublet by the first A nucleus and each of the doublet signals split again by the second A nucleus (Fig. 2.5b, (1) and (2)). Because the A nuclei are magnetically equivalent, the size of the  $J_{AX}$  coupling will be identical, and the doublets will add up to yield a triplet for the X resonance with an intensity ratio 1:2:1 (Fig. 2.5b, (1)). In the case of three magnetically equivalent X nuclei coupled to a single A (Fig. 2.5a, (1)), following the same reasoning above the A resonance will be split into four lines of intensity 1:3:3:1 (Fig. 2.5b, (1) and

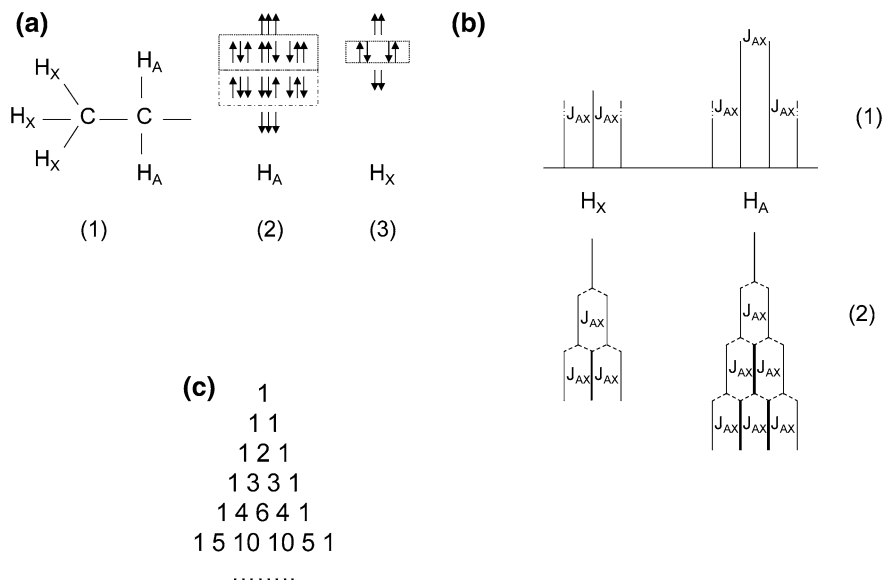


**Fig. 2.5** Splitting in a system with spin- $1/2$  nuclei. **a** Left (1): scheme of the molecule with three equivalent  $H_X$  nuclei and two equivalent  $H_A$  nuclei. Middle (2): the different possible orientations for the  $H_A$  due to the presence of  $H_X$  ( $2^3 = 8$ ). The orientations marked with a dotted square on one side, and those with a dash-and-dot square on the other are equivalent, because the spin orientations within each set of spins within a square are indistinguishable. Right (3): possible orientations for the  $H_X$  caused by the presence of  $H_A$  ( $2^2 = 4$ ). The orientations marked with a dotted square are equivalent, because the spins are indistinguishable. **b** Top (1): the resulting spectra for each of the  $H_A$  and  $H_X$  nuclei are shown. Bottom (2): diagram showing how the lines of the multiplets above are generated. Lines with different width indicate the overlapping of two or more lines of the multiplet. The separation between the lines corresponds to the coupling  $J_{AX}$ . **c** The Pascal triangle provides the intensity of each of the lines in the multiplet. Each number in a line of the triangle is the result of the addition of the numbers immediately above it

(2)), with the quantum states with several nuclei in alternate orientations having identical occupations (Fig. 2.5a, (2)). The general rule is that  $N$  magnetically equivalent spin- $1/2$  nuclei will split the resonance of a nearby spin (or group of spins) into  $N+1$  lines with a distribution intensity given by the Pascal triangle (Fig. 2.5c). If the spins involved do not have  $I = 1/2$ , then the number of split lines is  $2IN + 1$ . It is important to note that there is no coupling among the three  $H_X$  since they are magnetically equivalent (and the same is true for the two  $H_A$ ).

The above rules for signal multiplicities only apply for so-called *weak coupling*. This occurs when the chemical shift difference between the coupled nuclei is very large compared to  $J$  (Fig. 2.6, top spectrum). In the case of weak coupling, the flipping of one spin does not result in a tendency of the other spin to flip, and discrete resonance lines can be assigned to one or the other. The interested reader can look into this topic in more advanced NMR books or reviews (Günther 1995; Sternhell 1969; Barfield et al. 1990; Homans 1989). When the chemical shift

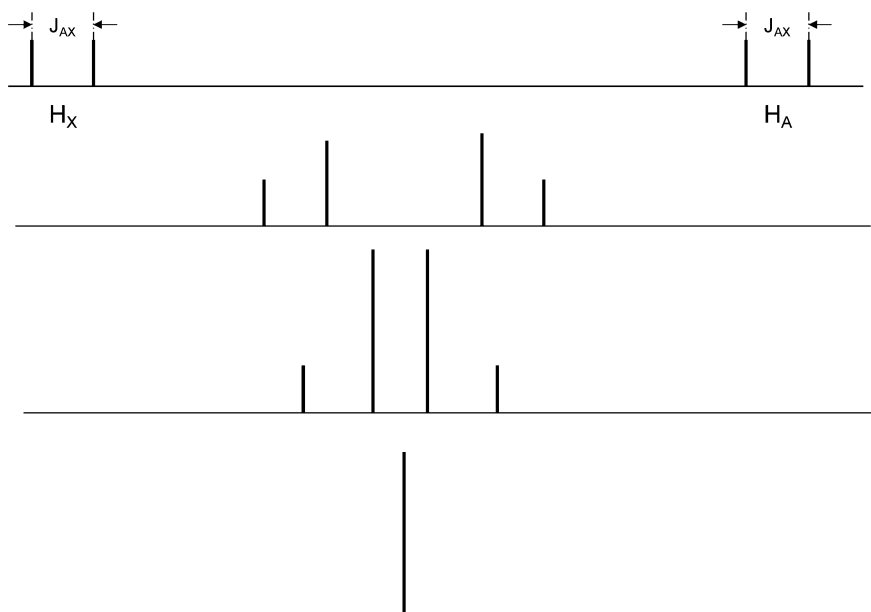


**Fig. 2.6** From weak to strong coupling. In the *top* spectrum the chemical shift separation between the A and X nuclei is much larger than the  $J_{AX}$ . In the second spectrum from the *top*, the  $J_{AX}$  is half the size of the chemical shift separation between the two nuclei. In the third spectrum, the  $J_{AX}$  and the chemical shifts are very similar. For magnetically equivalent nuclei (*bottom* spectrum) only one line with double intensity is observed. As the difference in chemical shift decreases, the inner lines increase in intensity while the  $J_{AX}$  is kept constant (the so-called *roof effect* is clearly observed in the second and third spectra)

difference between the two nuclei involved is not very large compared to the  $J$ , the rules no longer apply, and they are considered to be *strongly coupled*. This strong coupling distorts the intensities of the simple doublets between two coupled protons in the NMR spectrum, giving rise to the situation known as the *roof effect* (Fig. 2.6, second and third spectra from the top). In this situation, the intensities of the outer resonances decrease while the inner ones increase, reaching a limit where the two coupled protons are identical (magnetically equivalent) and a single resonance is observed for both (Fig. 2.6, bottom spectrum).

### 2.2.2 How Does Spin–Spin Coupling Occur?

Spin–spin coupling is mediated via the electrons of covalent bonds, and therefore its magnitude decreases rapidly as the number of intervening bonds increases. The basic mechanism that propagates coupling is polarization. If there is a coupling between the electron and the nucleus, the polarization may be: (i) a dipolar

interaction between the electron and the nucleus; or (ii) a *Fermi-contact* interaction (an interaction that depends on the proximity of an electron to the nucleus, and hence only observed in s-orbitals occupied by electrons). This latter interaction between electrons and nuclei does not necessarily imply that both particles must be antiparallel or parallel, as the arrangement depends on the type of atom involved in the bond. If we consider two spin- $\frac{1}{2}$  nuclei, A and B, linked by an electron-pair bond and presenting a scalar coupling  $^1J_{AB}$ , the molecular orbital between the atoms will be occupied by the two electrons of the bond, which according to Pauli's principle, will present an antiparallel spin arrangement in the orbital. The nuclear spin B can have a spin parallel or antiparallel to the spin of the second electron depending whether it is in the  $\alpha$  or  $\beta$  state (Fig. 2.7a). If we assume that parallel arrangements of spins (nuclear and electrons) have a higher energy than the antiparallel ones, then two conformations are possible (and hence give rise to a doublet). The same occurs when the transmission through the bond is explained from the point of view of nucleus B. A stronger Fermi interaction will occur when the percentage of *s-orbitals* in the intervening bond is larger. For instance, for  $^1J(\text{H-}^{13}\text{C})$ , the higher the percentage of s-orbital in the hybrid orbital, the larger the spin-spin coupling constant will be, going from around 250 Hz in sp-orbitals to approximately 140 Hz in hybrids  $\text{sp}^3$  (Günther 1995). From the above discussion, it is clear that the coupling of a nucleus to an electron via the Fermi-contact interaction is important for protons, but not necessarily relevant for other nuclei. Heavier nuclei interact through other processes like the dipolar mechanism between the electron magnetic moment and their orbital motion.

When we consider the coupling between atoms via two bonds ( $^2J_{AB}$ ), as in H-C-H (geminal protons), we need to take into account a mechanism which “transmits” spin alignment through the central C atom. In the example shown in Fig. 2.7b, the H atom (A) polarizes the nearest electron with an antiparallel arrangement, and consequently the other electron occupying the same molecular

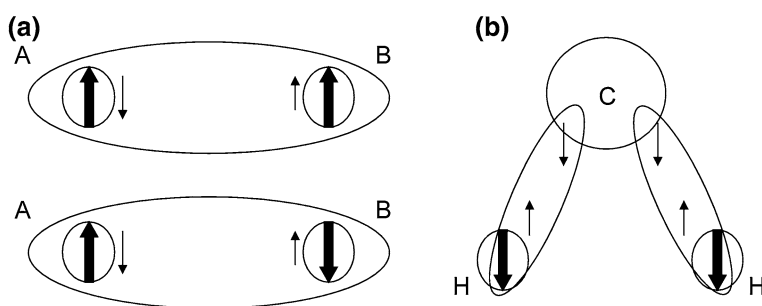


**Fig. 2.7**  $^1J$  and  $^2J$  couplings. **a** The polarization mechanism for the spin-spin coupling ( $^1J_{AB}$ ). The information is transmitted through the Pauli's principle, and the two possible arrangements shown have different energies. **b** The polarization mechanism for  $^2J_{HH}$  spin-spin coupling. The coupling information is transmitted from one bond to the next taking into account the Hund's rule of maximum multiplicity. In both (a) and (b) panels the nuclear spins are shown by thick *black arrows* and the electrons by thin *arrows*

orbital, likely to be close to the carbon, will also have an antiparallel arrangement (Pauli's principle). The carbon atom shares another electron with the second H atom; according to Hund's rule, the electrons closer to the carbon, in both C–H bonds, must have parallel orientations. In the second C–H molecular orbital, the electrons must have an antiparallel arrangement according to Pauli's principle, and therefore, the energy of the second H nucleus (atom B) is the result of the spin arrangement with its closest electron. Of course, the value of the interaction (and hence, the magnitude of  $^2J$  and its sign) will depend on the hybridization of the carbon atom.

### 2.2.3 Variations in the Value of $J$

We shall describe briefly how the spin–spin coupling constant varies according to chemical and structural factors. We shall focus on couplings involving protons, since the body of literature on that nucleus is comprehensive (Günther 1995; Sternhell 1969; Barfield et al. 1990; Homans 1989).

(a) *Geminal couplings* ( $^2J$ ). This corresponds to the coupling between two protons bound to the same carbon atom. Values rely heavily on the hybridization of the carbon nuclei to which both H nuclei are bound and on the presence of electronegative substituents. To be able to observe the coupling between two protons, they must experience different magnetic environments. The range of  $^2J$  values varies from 12–20 Hz in geminal protons in alkanes to 0–3.5 Hz in geminal protons in alkenes (Günther 1995).

(b) *Vicinal couplings* ( $^3J$ ). The coupling between protons separated by two carbon (or other) atoms. The value of this coupling constant depends on: (i) the presence of electronegative substituents; (ii) the distance between the two carbons involved ( $r_{CC}$ ); (iii) the HCC valence angles ( $\Theta_1$  and  $\Theta_2$ ); and (iv) the dihedral angle between the C–H bonds under consideration ( $\phi$ ) (Fig. 2.8a). Perhaps the most distinctive feature is the variation with the  $\phi$  angle, which varies with the expression:  $^3J = A + B\cos(\phi) + C\cos(2\phi)$ , where A, B and C are constants that depend of the nuclei involved (Fig. 2.8b). This mathematical expression is known as the *Karplus equation* and its use requires the assumption that the dihedral angle adopts a prevailing value over time (that is, a single rotamer must be predominantly populated). If there is a rapid averaging of the dihedral angle (that is, the bonds are easily rotatable) an averaging of the possible coupling constants will be observed. The equation can be successfully applied to systems where the bonds cannot be rotated (in sugars, for instance, the vicinal coupling constant between the anomeric proton and its neighbour determines whether the sugar is  $\alpha$  or  $\beta$ ). The equation is explained by the fact that the overlapping efficiency of the molecular orbitals involved in “transmitting” the coupling is determined by the  $\phi$  angle.

(c) *Long range couplings* ( $^nJ$ ,  $n \geq 4$ ). Although generally small in size,  $^nJ$  couplings are frequently observed. They normally produce very small splittings, which are observed at high magnetic fields. Currently, splits of 0.2 Hz or even

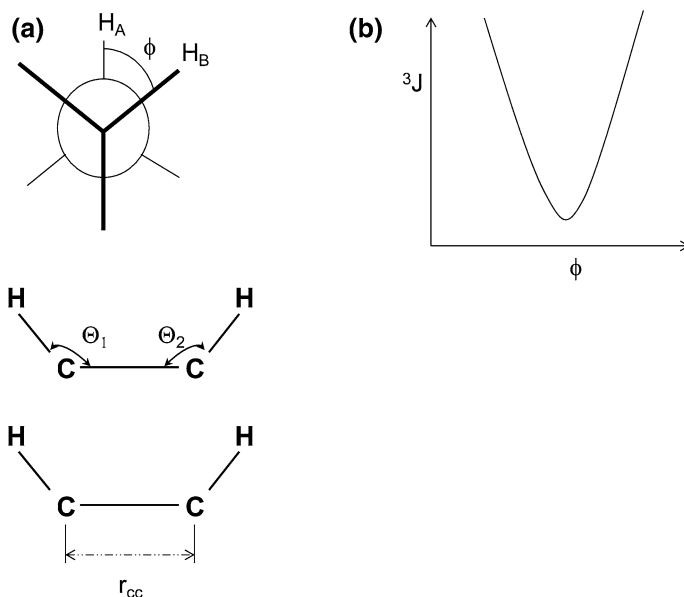


**Fig. 2.8** Variation of  $^3J$ . **a** Factors on which  $^3J$  depends (from *top to bottom*): dihedral angle ( $\phi$ ), valence angles ( $\Theta$ ) and the carbon-carbon distance ( $r_{cc}$ ). **b** The Karplus curve (the angles must be measured in radians) shows the variation of  $^3J$  according to the dihedral angle

lower can be easily detected, and in general the  $^4J$  values are in the range 0.1–3 Hz, although larger values are not unusual. They are commonly observed in saturated atoms which are coplanar or in a W-shaped conformation, and also in atoms involving  $\pi$ -orbital bonding. Although in principle  $\pi$ -electrons do not propagate scalar couplings because  $\pi$ -orbitals have nodes (no electronic density) at the position of the nuclei,  $^4J$  can be measured in these systems due to the high delocalization of the electronic density. A further description of the mechanism of transmission in these coupling constants through the bonds is beyond the scope of this chapter but the interested reader can find further details in the literature (Günther 1995).

### 2.2.4 Spin–Spin Decoupling

Spin–spin coupling yields important chemical information about the number of nuclei surrounding a particular observed nucleus, but they also complicate the NMR spectra by increasing the number of lines. Therefore, techniques used for eliminating spin–spin coupling are of considerable importance, and are routinely used in 1D, 2D and nD-NMR experiments (Chaps. 3 and 4). Decoupling can be applied to the  $^1H$  nucleus when collecting, for instance,  $^{13}C$  spectra, but the

scheme is of general applicability to any other nuclei. An in-depth description of available decoupling techniques can be found in the literature (Freeman 1997).

Spin–spin decoupling rests on the application of a second radiofrequency source, in addition to the transmitter frequency used for the recording of the main spectrum. If we consider a spin system formed by two spins A and B showing a  $J_{AB}$  coupling, a normal spectrum will present a doublet for each of the spins. If during the recording of the NMR spectrum we irradiate at the precise frequency of, for instance, the B nucleus with the second transmitter, the effect will be the disappearance of the coupling at the A frequency which will show a single line. During the irradiation at B, this nucleus is switched around by the decoupling field so fast (compared to  $J$ ), that the A spins only “see” the average of the B spin, that is, the probability of an upward transition in B is the same as for a downward transition, with the result of the B multiplet being saturated (Chap. 1). An example of the decoupling technique is shown in the inset of Fig. 2.1 where the  $\text{CH}_2$  signal of ethanol has been decoupled (the bolt). In this case, the saturation of the methylene resonance removes the splittings from the coupled signals, yielding two singlets for both the  $\text{CH}_3$  and OH signals.

Although decoupling is a very useful NMR technique, it can also cause problems. Incomplete decoupling leads to signal broadening, imperfect selectivity of the irradiated signal leads to decoupling of neighbouring resonances, changes in the chemical shift of the signals close to the irradiation peak (Bloch-Siegert shifts) and population alterations which can vary the intensity of some resonances due to, among others, NOE effects.

## 2.3 The Nuclear Overhauser Effect

In the Sect. 2.2 we have described the scalar couplings between nuclei: indirect couplings are transmitted through the electrons intervening in the chemical bonds. In this section, we shall be dealing with another class of coupling: the dipolar coupling that gives rise to the *nuclear Overhauser effect* or *NOE*. The effect is described simply by considering a system formed by two spins A and X, which do not show spin–spin scalar coupling, but are spatially close enough to interact by means of a dipole-dipole interaction (Chap. 1). In the NMR spectrum of such system we should expect two lines, one from A and another from X. If we irradiate the system with a radiofrequency at the resonance frequency of X, providing that enough power is used to saturate the transition (that is, the populations of the X levels are equal, Chap. 1), we shall observe that the intensity of the A resonance is modified: enhanced, diminished or even converted into an emission line rather than an absorption one. This modification is the NOE.

The NOE measurement is crucial to the determination of the conformation of molecules. This information can be obtained because the NOE depends, among other factors, on the distance between the nuclei involved. The NOE effect is also used as a way of enhancing the sensitivity of low- $\gamma$  nuclei. For instance, the



decoupling of  $^1\text{H}$  during the recording of  $^{13}\text{C}$  spectra, contributes to an increase in the  $^{13}\text{C}$  signals by means of the NOE effect between each carbon and its attached protons. We shall describe in this section the basis and main applications of the NOE, but for a full description of the matter, the interested reader is directed to the comprehensive text by Neuhaus and Williamson (Neuhaus and Williamson 1999) which also includes important applications of the NOE in the study of biomolecules.

For the description of the NOE background, how the effect arises and what factors determine its sign and magnitude, we shall restrict our discussion to *steady-state* NOEs. In these NOEs, the perturbation is brought about by saturating one of the spins via the selective application of a weak radiofrequency irradiation at the frequency of that particular spin resonance. This is the kind of NOE observed in the well-known method among chemists, as the NOE-difference. We shall begin the discussion by considering the simplest example of a homonuclear spin- $1/2$  system, and from there we will extend to more representative multispin systems. Further details and the kind of experiments used will be described in Chaps. 3 and 4.

### 2.3.1 The Basis of the NOE: A Two-Spin System

To be able to understand the NOE, we need to think in terms of energy level populations. In an AX system formed by two spins which are not scalarly coupled, there will be four energy levels (Fig. 2.9a). At equilibrium, the population of the  $\alpha_A\alpha_X$  state is the largest, and that of the  $\beta_A\beta_X$  state is the lowest, with the other two levels showing the same energy and an intermediate population. The intensities of the peaks in the NMR spectrum (Fig. 2.9a, bottom) reflect the population in each of the levels (Chap. 1). When the X transitions are saturated (Fig. 2.9a, bolts), the populations of the X levels become identical, but no changes are observed in the population of the A levels (Fig. 2.9b). In a system with two isolated spins, this X saturation would cause in the spectrum the loss of the X resonance and no effect whatsoever on the A resonance (Fig. 2.9b, bottom). However, in our dipolarly coupled A-X system we have to take into account the relaxation effects between the two spins (Chap. 1). Since the system has been forced away from equilibrium by altering its level populations, it will be inclined to strive to regain the original state by recovering those spin populations in each level via relaxation processes.

Relaxation can occur in several ways if dipolar interactions exist between the A and X spins. However, to be observed in an NMR experiment, the process must correspond to a single-quantum transition. This process involves a net change of quantum moment of 1, that is, it implies the flip of a single spin (A or X), as for example from  $\alpha_A\alpha_X$  to  $\beta_A\alpha_X$ . There are two of these processes in the system (Fig. 2.9c). However, there are another two additional relaxation processes by which the system can regain the equilibrium population. For instance, another relaxation possibility is for an active field to cause both spins to flip concomitantly from  $\beta$  to  $\alpha$ , and therefore, the  $\alpha_A\alpha_X$  and  $\beta_A\beta_X$  levels will regain their equilibrium

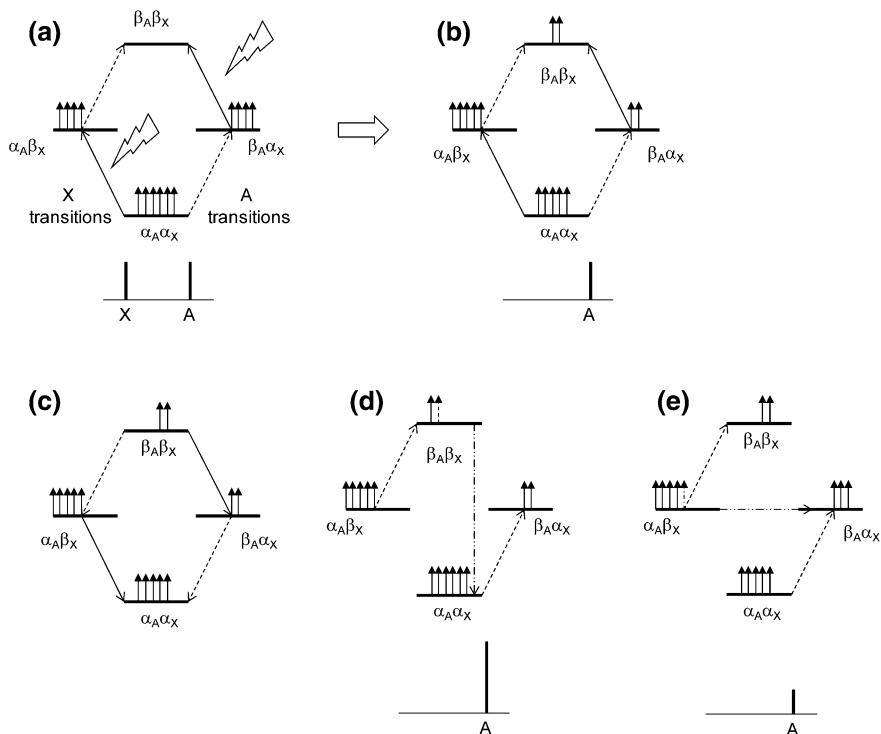


**Fig. 2.9** The NOE. **a** The energy levels of an AX system and an indication of their relative populations. The transitions involving the changes in the A spin are indicated by dashed arrows while those involving the change in the X state are shown as continuous arrows. The bolts indicate the transitions being saturated (those of nucleus X). The corresponding spectrum is shown at the bottom. **b** Energy levels after saturation of the X transitions. The bottom of the figure shows the resulting spectrum. **c** Single-quantum transitions, which could induce the recovery of the equilibrium populations. The continuous or dashed arrows have the same meaning as in panel (a), but their direction is opposite (with the arrow head pointing towards the lower energy level). **d** The double-quantum transition is shown as a dot-and-dash arrow. The dotted spin in the highest level indicates the one which is transferred at the lowest level; now the transitions (dashed arrows) involving the A spin are more intense because there are more spins in the basal A levels than in the equilibrium situation (panel (a)). The bottom of the figure shows the resulting spectrum (positive NOE). **e** The zero-quantum transition is shown as a dot-and-dash arrow. The dotted spin in the medium level indicates which one is being transferred; in this case, the transitions (dashed arrows) involving the A spin are less intense (because there are fewer spins in the basal A levels) than in the equilibrium situation (panel (a)). The bottom of the figure shows the resulting spectrum (negative NOE).

populations. This is called a two-quantum transition, since the orientation of the two spins change concomitantly and two quanta are changed. This transition cannot be observed directly in an NMR experiment, as there is a net change of two in the total quantum moment (the transition is said to be forbidden by quantum mechanics rules) (Fig. 2.9d). However, this spin flipping leaves the populations of

the saturated  $\alpha_A\beta_X$  and  $\beta_A\alpha_X$  unaltered; therefore, the population difference between the states joined by changes in the spin A are now larger than at equilibrium (there are more spins in the basal state). As a consequence, the intensity of the resonance absorption will be enhanced (Fig. 2.9d, bottom). This condition represents a NOE effect where the difference in intensity results in signal enhancement.

The last possible relaxation mechanism between the levels is the dipolar interaction causing  $\alpha$  to flip to  $\beta$  and  $\beta$  to flip to  $\alpha$ , or the  $\alpha_A\beta_X - \beta_A\alpha_X$  transition. This zero-quantum transition (the net change of quantum moment is null) is not observed directly in the NMR experiment either (Fig. 2.9e). The zero-quantum transition equilibrates the populations of  $\alpha_A\beta_X$  and  $\beta_A\alpha_X$  but leaves the populations of  $\alpha_A\alpha_X$  and  $\beta_A\beta_X$  unaltered. In this case, the population difference between the states involving changes of the spin A is smaller than at equilibrium and the intensity of the resonance absorption will be diminished: in this NOE effect, the difference in intensity results in signal decrease (Fig. 2.9e, bottom).

In practice, the effect lies somewhere between these two limits, and it is usually reported in terms of the  $\eta(X)$  (being X the saturated nucleus):  $\eta(X) = \left(\frac{I-I_0}{I_0}\right)$ , where  $I_0$  is the intensity of the resonance in the absence of any saturation and  $I$  is the NOE intensity of a particular transition. From the above considerations, it is clear that the building-up of a NOE (either negative or positive) will depend on the different contributions of the zero- or double- quantum processes (the so-called *cross-relaxation* processes). If the double-quantum contribution dominates, the NOE will be positive, whereas it will be negative if the zero-quantum relaxation contributes most. In addition, the single-quantum relaxation processes (those shown in Fig. 2.9c) will re-establish the equilibrium once the saturation has been removed, and therefore will compete with both cross-relaxation processes. If these single-quantum processes are efficient enough, NOEs will fail to develop.

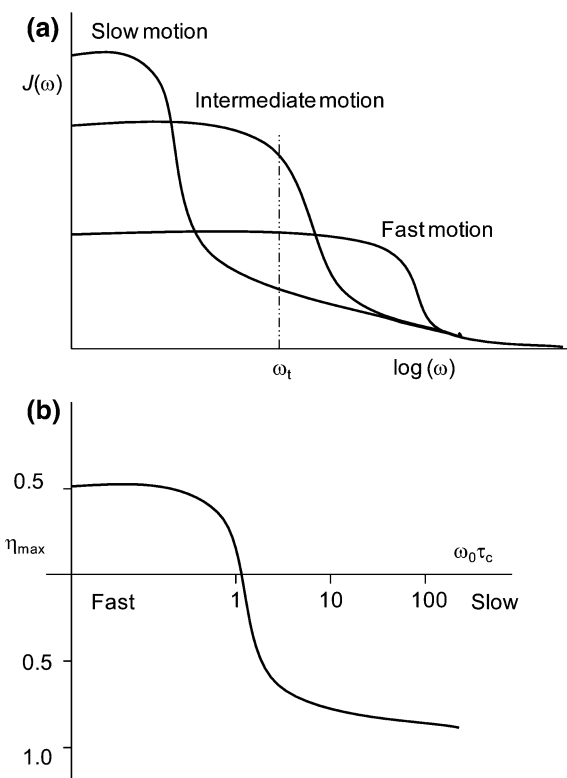
To summarize all of the above, we can define the NOE as the result of a balance of different competing relaxation pathways.

### 2.3.1.1 The Dipolar Coupling and the Tumbling of the Molecule

Nuclear spins suffer relaxation processes caused by local-field oscillations at a frequency close to their Larmor frequencies (Chap. 1). These variations originate, in most cases, with the tumbling of the molecule in solution (defined by the correlation time,  $\tau_c$ , Chap. 1). The tendency within a molecule to induce quantum transitions by means of its molecular tumbling is called *spectral density*, and is represented as  $J(\omega)$ . The spectral density can also be viewed as the probability of a component of the motion of the molecule being at a particular frequency. Therefore, relaxation can only occur when a frequency exists at the Larmor frequency of the particular spin, out of the whole set of frequencies that are explored by the molecule (and which are given by  $J(\omega)$ ).

The spectral density function has the general form  $J(\omega) = \left( \frac{2\tau_c}{1+\omega^2\tau_c^2} \right)$  (Levitt 2009), and the shape it adopts, depending on the value of  $\tau_c$ , is shown in Fig. 2.10a. For molecules which tumble slowly (long  $\tau_c$ , slow motion) there is a very small probability of finding frequencies of rapidly oscillating fields (that is, the  $J(\omega)$  curve has a small area at the largest frequencies). For instance, for a transition occurring at a frequency  $\omega_t$  (Fig. 2.10a) the probability of finding oscillating fields in molecules with slow motions is very small; the probability of finding species with the proper frequency will be larger only in molecules with intermediate motions (second curve in Fig. 2.10a). Using these arguments, it is possible to predict whether the zero- or double-quantum processes will be dominant in the NOE building-up. In the zero-quantum process, the energy differences between the two frequencies for the A and X spins are small (in fact, we have assumed above that the  $\alpha_A\beta_X$  and  $\beta_A\alpha_X$  were degenerate). Therefore, the particular  $\omega_t$  will be on the left-hand side of the x-axis of  $\log(\omega)$  (since in a zero-quantum transition, the  $\omega_t = \omega_A - \omega_X$ ) and we should be able to find a large number of fluctuating fields with that proper small frequency for molecules with slow motion. The relaxation mechanism governed by the zero-quantum transitions is predominant in molecules with long  $\tau_c$ , which will give rise to negative NOEs.

**Fig. 2.10**  $J(\omega)$  and NOE curves. **a** Schematic  $J(\omega)$  for three molecules tumbling with different motional regimes as a function of the frequency  $\omega$ ;  $\omega_t$  represents the frequency of the transition. **b** Variation of the maximum theoretical homonuclear steady-state NOE in a two-spin system as a function of  $\omega_0\tau_c$



Double-quantum transitions are likely to have very large  $\log(\omega)$  values since  $\omega_t$  will be the sum of the A and X frequencies,  $\omega_t = \omega_A + \omega_X$ , and will be located on the right-hand side of the x-axis of  $J(\omega)$ . Therefore, the probability of finding spins with the proper oscillating frequency will be higher in molecules with fast motion (short  $\tau_c$ ). Molecules with fast tumbling in solution will exhibit the double-quantum process as the main relaxation mechanism and give rise to positive NOEs.

Quantitative calculations show that the cross-relaxation rates not only depend on the  $\omega_A \pm \omega_X$  values, but also on  $\gamma_A$ ,  $\gamma_X$  and  $r^{-6}$ , where  $r$  is the distance separation between the two dipoles (A and X nuclei). This distance dependence comes from the variation of the dipolar relaxation rates (Chap. 1, Fig. 1.3), and causes the NOE to decrease sharply with distance. In practice, only NOEs between nuclei within 5–6 Å of each other will develop. The fact that cross-relaxation rates rely on the gyromagnetic constants of both spins means that very different rates can occur in heteronuclear systems. This is why decoupling of protons during the acquisition of  $^{13}\text{C}$  spectra yields NOE enhancements of nearly 200 % ( $\gamma_H \approx 4\gamma_C$ ), equivalent to a three-fold intensity increase of the  $^{13}\text{C}$  signal. In heteronuclear systems, the observed NOEs will also depend on the sign of the gyromagnetic ratios involved, and in the case of fast tumbling molecules, the NOEs from protons to nuclei with  $\gamma < 0$  can yield negative NOE values.

In a homonuclear system, the variation of the steady-state NOE ( $\eta$ ) with the molecular motion, expressed by the product of  $\omega_0\tau_c$  (where  $\omega_0$  is the spectrometer frequency) follows the curve shown in Fig. 2.10b. Since  $\omega_0$  is constant, the curve shows the variation with the tumbling of the molecule: if  $\tau_c$  is very long (the molecule tumbles slowly), we get negative NOEs. On the other hand, if the molecule tumbles very fast (short  $\tau_c$ ) the NOE becomes positive, which in NMR terminology is called the *extreme narrowing limit*. In the intermediate tumbling region, the NOE changes signs and will approach zero when the double- and zero-quantum relaxation mechanisms are equal. In this intermediate region the magnitude of the NOE is highly sensitive to the solution conditions (viscosity, temperature, pH or ionic strength) as well as the shape of the molecule. In fact, for some medium-size molecules the NOE will be too weak to be observed. In these cases, it is advisable to change the experimental conditions. Changing the field strength (i.e.  $B_0$ , which results in changes of  $\omega_0$ ) is not always feasible; alternatively, it is possible to use NOE experiments based on the rotating-frame, which always yield positive NOEs (Neuhaus and Williamson 1999; Levitt 2009) as will be explained in Chap. 4.

### 2.3.2 NOEs in Multispin Systems

The above discussion on a two-spin system assumes that the main mechanism of relaxation occurs through dipole–dipole relaxation. However, the presence of other spins influences the NOE build-up and the cross-relaxation mechanisms by the

intervention of other competing relaxation processes ([Chap. 1](#)). Thus, two spins showing a strong dipolar coupling due to their proximity might not produce a large NOE if other neighbours are available to compete. We shall further comment on these effects in [Chap. 3](#), but the interested reader can also have a look at selected literature (Neuhaus and Williamson [1999](#); Kalk and Berendsen [1976](#); Cavanagh et al. [1996](#)).

Finally, the build-up of NOEs can be affected by *chemical-exchange* processes. Exchange processes are chemical reactions that take place within the same molecule or with other chemical entities in solution. The involvement of some spins in exchange processes, and also in the building-up of the NOE, translates into saturation transfer processes. For instance, a saturation transfer can occur when a molecule suffers a conformational-exchange reaction (e.g. conformer equilibrium of sugar rings), where saturation of a spin transition in one conformer can lead to saturation in the other conformer.

## References

- Barfield M, Collins MJ, Gready JE, Hatton PM, Sternhell S, Tansey CW (1990) NMR studies of bond orders. *Pure Appl Chem* 62:463–466
- Cavanagh J, Fairbrother WJ, Palmer AG 3<sup>rd</sup>, Skelton N (1996) *Protein NMR spectroscopy. Principles and practice*, 1<sup>st</sup> edn. Academic Press, New York
- Freeman R (1997) *Spin choreography: basic steps in high resolution NMR*. Spektrum, Oxford
- Günther H (1995) *NMR spectroscopy: basic principles, concepts and applications in chemistry*, 2nd edn. Wiley and Sons, New York
- Homans SW (1989) *A dictionary of concepts in NMR*. Clarendon Press, Oxford
- Kalk A, Berendsen HJC (1976) Proton magnetic relaxation and spin diffusion in proteins. *J Magn Reson* 24:343–366
- Levitt MH (2009) *Spin dynamics: basis of nuclear magnetic resonance*, 2nd edn. Wiley, Chichester
- Neuhaus D, Williamson MP (1999) *The nuclear Overhauser effect in structural and conformational analysis*, 2nd edn. VCH Publishers, New York
- Sternhell S (1969) Correlation of interproton spin–spin constants with structure. *Q Rev Chem Soc* 23:236–270
- Wishart DS, Bigam CG, Yao J, Abildgaard F, Dyson HJ, Oldfield E, Markley JL, Sykes BD (1995) <sup>1</sup>H, <sup>13</sup>C and <sup>15</sup>N chemical shift referencing in biomolecular NMR. *J Biomol NMR* 6:135–140

NMR for Chemists and Biologists

Carbajo, R.J.; Neira, J.L.

2013, XII, 115 p. 36 illus., Softcover

ISBN: 978-94-007-6975-5